Original Article

Pharmaceutical Sciences and Research (PSR), 10(3), 2023, 139 - 150

Molecular Docking Analysis of *Acanthus ilicifolius* Compounds Toward CUL4B-DDB1-AhR-ERα Complex Protein for Antiosteoporosis Discovery

Binar Asrining Dhiani[1*], Sarmoko[2], Retno Wahyuningrum[1], Akbar Yulianto[1]
[1]Faculty of Pharmacy, University Muhammadiyah Purwokerto, Central Java, Indonesia
[2]Department of Pharmacy, Faculty of Science, Sumatera Institute of Technology, South Lampung, Indonesia

ABSTRACT

Osteoporosis represents a significant global public health issue, particularly among the aging population. Its incidence reaches 18.3% of the total population, with the highest prevalence observed in elderly postmenopausal women. A key factor in osteoporosis is the decreased expression level of estrogen receptor alpha (ERα), attributed to its degradation by the ubiquitin ligase protein complex Cullin4B (CUL4B), DNA damage binding 1 (DDB1), and aryl hydrocarbon receptor (AhR), collectively known as CUL4BAhR. *Acanthus ilicifolius L* contains compounds exhibiting antiosteoporosis activity, primarily by inhibiting osteoclastogenesis via RANKL. However, no reports exist of antiosteoporosis agents that act by inhibiting ERα degradation via CUL4BAhR. This study employed an *in silico* approach to predict active compounds from *A. ilicifolius* that could inhibit ERα degradation via CUL4BAhR, potentially developing them into antiosteoporosis agents. We utilized the 3D structures of proteins CUL4B-DDB1 (PDB ID:4A0L), AhR (5NJ8), and ERα (1A52) in various molecular docking tools, including ClusPro2.0, PyRx0.8, PyMol, PLIP, and SWISS-MODEL for QMEAN and structure assessment analysis. The ligands tested were acancifoliuside, acanthaminoside, acteoside, isoacteoside, (-)-lyoniresinol, (-)-lyioniresinol-3a-O-β-glucopyranoside, and estradiol. Acteoside displayed lower binding affinity energy (-9.7 kcal/mol) compared to estradiol (-8.9 kcal/mol) and was the lowest among all compounds. Acteoside was found to weaken the interaction between CUL4B-Rbx1 and CUL4B-DDB1 but not between AhR and ERα. Consequently, acteoside could be a viable candidate as an antiosteoporosis agent by inhibiting ERα degradation via the CUL4B-DDB1-AhR pathway. Further biochemical, *in vitro*, and *in vivo* studies are required to strengthen this evidence.

ARTICLE HISTORY

Received: September 2023
Revised: December 2023
Accepted: December 2023

Keywords: *Acanthus ilicifolius; antiosteoporosis; CUL4B-DDB1-AhR; ERa; estrogen receptor*

**corresponding author*
Email:binar_dhiani@ump.ac.id

INTRODUCTION

Osteoporosis represents a significant public health issue globally, particularly in the aging population. By 2030, it is estimated that the number of people aged 60 and over will reach 1.4 billion (WHO, 2023). The prevalence of osteoporosis is currently at 18.3% across the entire population, with the highest incidence found in elderly postmenopausal women. Additionally, it has been reported that 20% of women with osteoporosis suffer from fatal hip fractures (Salari et al., 2021).

Osteoporosis is characterized by increased osteoclastogenesis, reduced osteoblast activity, and an imbalance in bone remodeling (Hendrijatini et al., 2019). During postmenopausal conditions, estrogen levels decrease. Estrogen interacts with estrogen receptor alpha (ERα), playing a crucial role in osteoblast generation, inhibiting bone resorption and osteoclastogenesis (Khalid & Krum, 2016). The reduction in ERα expression in postmenopausal women leads to an increase in the level of the receptor activator of NF-κB ligand (RANKL) and a decrease in osteoprotegerin (OPG), thereby stimulating osteoclast differentiation (Lee et al., 2013; Shen et al., 2022; Streicher et al., 2017).

The decline in ERα levels is attributed to its degradation by a ubiquitin ligase complex, comprising cullin4B (CUL4B), DNA damage binding 1 (DDB1), and the aryl hydrocarbon receptor (AhR) (Lee & Zhou, 2012; Ohtake et al., 2009, 2011, Dhiani & Mehellou, 2020). The CUL4BAhR ubiquitin ligase complex recruits and degrades ERα (Ohtake et al., 2011).

Certain plants contain glycoside compounds structurally similar to estrogen, demonstrating estrogenic activity via estrogen receptors and possessing antioxidant properties, such as soy and *Pueraria mirifica* (Jia et al., 2012; Jungsukcharoen et al., 2014). These glycoside compounds are reported to regulate proliferation and

osteoblast-osteoclast activities by inhibiting RANKL expression due to decreased ERα expression (Wu et al., 2022). Acteoside, a glycoside compound, along with steroids, alkaloids, and other flavonoid compounds (Bora et al., 2017; Saranya et al., 2015; Singh & Aeri, 2013; Van Kiem et al., 2008), is present in *Jeruju* (*A. ilicifolius*), a mangrove plant commonly found in Indonesia's coastal areas. Flavonoids, polyphenolic, and steroid compounds are found in the hydrolyzed-water fraction and its active subfraction (Dhiani & Andini, 2021). Acteoside inhibits osteoclastogenesis mediated by RANKL (Lee et al., 2013) and promotes the growth and differentiation of osteoblast cells MC3T3-E1 (Van Kiem et al., 2008), potentially preventing osteoporosis.

Several plants have been identified as potential antiosteoporosis agents (Jia et al., 2012). However, no existing reports reveal the potential of *A. ilicifolius* compounds as antiosteoporosis agents based on the molecular mechanism, specifically focusing on the inhibition of ERα degradation by the CUL4BAhR complex.

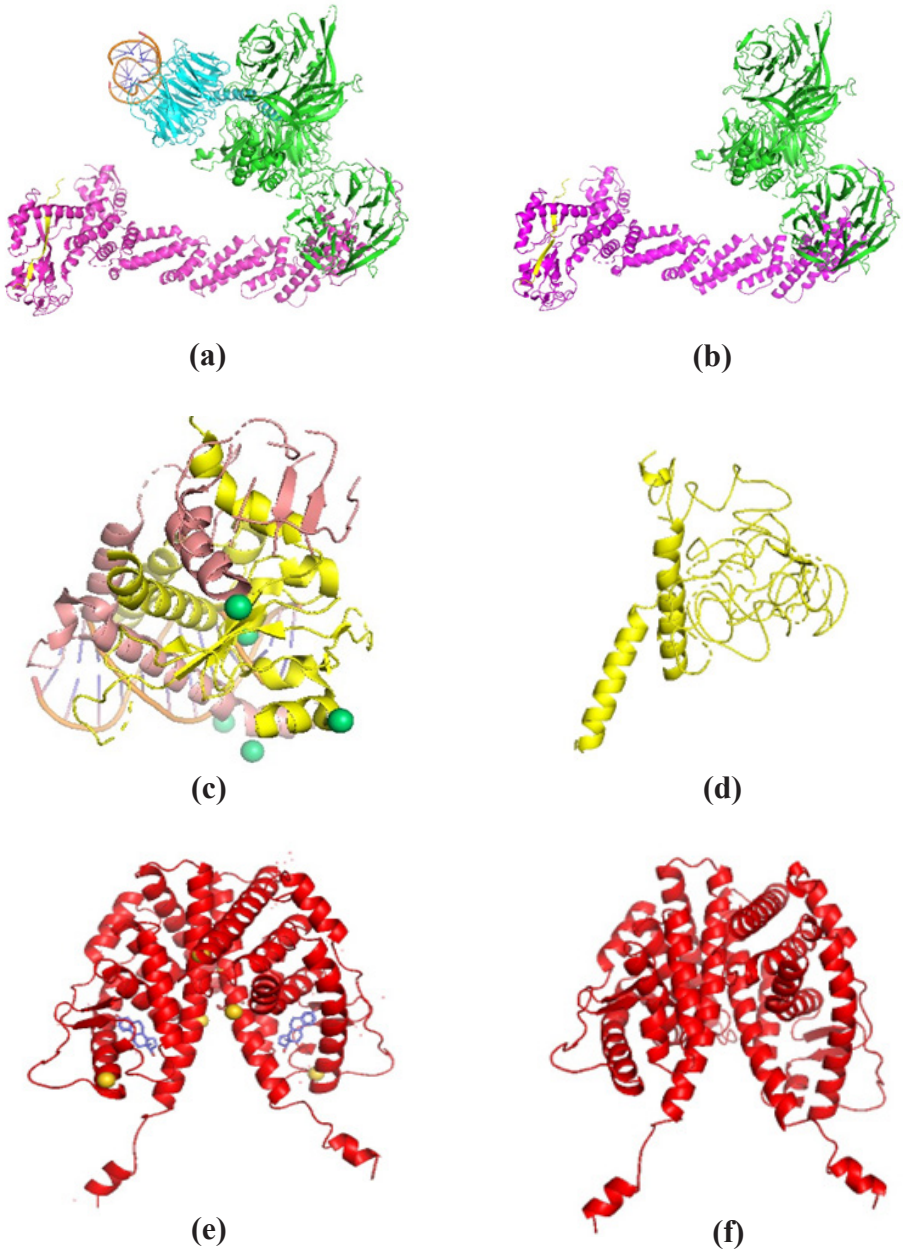

Figure 1. The 3D structure of proteins to build the CUL4B-DDB1-AhR-ERα complex structure. Rbx1-CUL4B-DDB1 complex (PDB ID: 4A0L) before (a) and after (b), AhR (PDB ID: 5NJ8) before (c) and after (d), and ERα (PDB ID: 1A52) before (e) and after (f) preparation process

In this study, we report on the molecular docking analysis of *A. ilicifolius* compounds on the CUL4B-DDB1-AhR-ERα complex using various tools, including Cluspro2.0, PyRx0.8, PyMol, PLIP, and SWISS-MODEL for QMEAN and structure assessment analysis.

METHODS

Protein and Ligand Preparation

The crystal structures of the Rbx1-CUL4B-DDB1 complex (PDB ID: 4A0L), AhR (PDB ID: 5NJ8), and ERα (PDB ID: 1A52) were obtained from the Protein Data Bank (https://www.rcsb.org/, 2022). Water and other ligands or macromolecules associated with the structures that were not used in this experiment (DDB2 and 12BP DNA Duplex in 4A0L; acetate ion, erbium ion, DNA, and aryl hydrocarbon receptor nuclear translocator in 5NJ8; EST and Au in 1A52) were removed. Hydrogen atoms were added to the proteins, and their geometry was cleaned using PyMol software. The structures were then saved as PDB files for uploading in ClusPro 2.0 (Kozakov et al., 2017) for protein-protein docking.

The compounds reported by Van Kiem et al. (2008) were used in this experiment. These include acancifoliuside, acteoside (CID 5281800), isoacteoside (CID 6476333), acanthaminoside, (+)-lyoniresinol-3a-O-β-glucopyranoside, (-)-lyoniresinol (CID 9888378), and estradiol (CID 5757). Molecule structures available in PubChem were retrieved as .sdf files, and those not available were drawn in ChemSketch, optimized for 3D geometry in 3D Viewer tools. Their energy was minimized and converted to .pdbqt format using Open Babel integrated into PyRx 0.8.

Protein-protein Docking of CUL4B-DDB1 and AhR

Protein-protein docking between CUL4B-DDB1 and AhR was conducted using ClusPro 2.0 (Kozakov et al., 2017). ClusPro 2.0 involved three computation steps: 1) rigid-body docking with billions of global protein conformations, 2) clustering 1000 structures with the lowest binding energy based on RMSD to model the cluster representation, and 3) sorting the structure with the minimum energy.

The 3D structures of the CUL4B-DDB1 complex (PDB ID: 4A0L) and AhR (PDB ID: 5NJ8), prepared as described above, were used as input for ClusPro 2.0. Four cluster models were obtained, with the model showing the lowest energy based on the "balanced" coefficient selected for visualization and analysis using PyMol 2.4.1 software.

Validation of the protein-protein docking results was conducted using QMEAN and structure assessment analysis on the .pdb file of the model showing the correct position of AhR in DDB1, using SWISS-MODEL (https://swissmodel.expasy.org/) and interaction analysis between amino acid residues in the complex was performed using the PIC web server (http://pic.mbu.iisc.ernet.in/cgi/submit_job.cgi) (Tina et al., 2007) and PDBePISA (https://www.ebi.ac.uk/msd-srv/prot_int/cgi-bin/piserver).

Protein-protein Docking of CUL4B-DDB1-AhR Complex and ERα

The best model of the CUL4B-DDB1-AhR complex, selected from the previous protein-protein docking step, was then docked to ERα using ClusPro 2.0, following the same analysis steps.

Table 1. Model score of the complex CUL4B-DDB1-AhR

Cluster	Members	Representative	Weighted Score
11	18	Center	-874.1
		Lowest Energy	-874.1
13	17	Center	-765.1
		Lowest Energy	-848.2
25	11	Center	-813.0
		Lowest Energy	-813.0

Table 2. QMEAN score, MolProbity score, and % highly favored region on ramachandran plot of selected models CUL4B-DDB1-AhR

Model	QMEAN Score	MolProbity Score	%Highly favored region on Ramachandran plot
11	-3.39	3.12	90.61
13	-3.44	3.10	90.36
25	-3.39	3.63	91.30

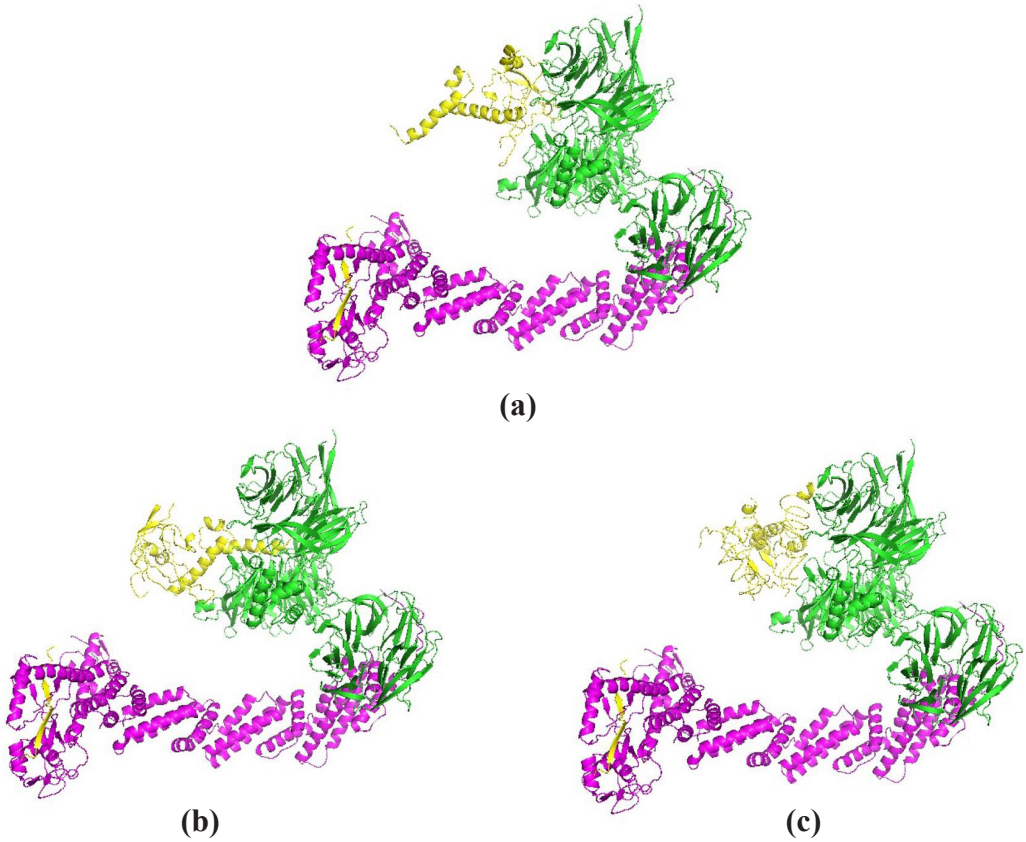

Figure 2. Visualization of complex protein CUL4B-DDB1-AhR model 11 (a), 13 (b), and 25 (c) generated from Cluspro 2.0

Table 3. Model score of the CUL4B-DDB1-AhR-ERα protein complex

Cluster	Members	Representative	Weighted Score
0	56	Center	-1153.0
		Lowest Energy	-1394.8
1	40	Center	-1143.9
		Lowest Energy	-1241.3
2	28	Center	-1011.0
		Lowest Energy	-1094.2
3	24	Center	-993.5
		Lowest Energy	-1401.7
4	23	Center	-1028.1
		Lowest Energy	-1256.5

Molecular Docking of Compounds to CUL4B-DDB1-AhR-ERα Complex

Molecular docking was performed to identify the *A. ilicifolius* compounds with the best binding scores using PyRx 0.8 (https://pyrx.sourceforge.io/) (Dallakyan & Olson, 2015). Utilizing AutoDock Vina integrated into PyRx 0.8, all seven compounds were docked against the predicted interface between AhR and ERα. Energy optimization of these molecules was carried out using the default energy minimization parameters provided by Open Babel within PyRx 0.8, employing the UFF force field and conjugate gradients as the optimization algorithm. The settings for 'total number of steps', 'number of steps for update', and 'stop if energy difference is less than' were configured to 200, 1, and 0.1, respectively (Dallakyan & Olson, 2015).

Table 4. Amino acid residues in the interface region between AhR and ERα

Types	AhR		ERα	
	Position	Residues with	Position	Residue
Hydrophobic interactions (within 5Å)				
	214	PRO	539	LEU
	214	PRO	543	MET
	215	LEU	536	LEU
	221	ILE	522	MET
	221	ILE	526	TYR
	227	LEU	462	LEU
	236	ALA	522	MET
	145	TYR*	358	ILE*
	146	LEU*	376	VAL*
	227	LEU*	461	PHE*
Hydrogen bonds				
Main chain-main chain				
	227	LEU	461	PHE
Main chain-side chain				
	227	LEU	377	HIS

Note: *new amino acid residue interaction after acteoside binds to the interface region

Subsequently, these compounds were converted into .pdbqt format, making them suitable for docking with the CUL4B-DDB1-AhR-ERα complex. The center of the grid box was set to coordinates (X: 18.7501, Y: 32.1680, Z: 69.9947), and its dimensions were X: 74.5658, Y: 87.0139, Z: 60.6323, with an exhaustiveness level of 8. The grid box size was chosen to encompass the interface area of AhR and ERα, which was identified as a potential binding site based on FTMap analysis (Figure 4.c) (Kozakov et al., 2015).

Docking validation involved re-docking estradiol from the native co-crystallized 1A52 structure to the CUL4B-DDB1-AhR-ERα complex in PyRx 0.8. This process began with manually opening the co-crystallized 1A52 file, followed by removing estradiol, which was then pasted and saved in PDB file format. The same protocol, including grid parameters, was maintained while docking this native estradiol with the CUL4B-DDB1-AhR-ERα complex. The re-docked estradiol was then superimposed onto the CUL4B-DDB1-AhR-ERα-estradiol complex, and the RMSD value was calculated using PyMol.

The ligand positioning within the CUL4B-DDB1-AhR-ERα complex was visualized using PyMol 2.4.1 software (https://pymol.org/2/). The docking calculations yielded binding affinity and RMSD values, which PyRx 0.8 automatically sorted to identify the lowest energy for each compound, with a standard limit of 2 Å. Interaction analysis between amino acid residues in the complex, both with and without the ligands, was then performed using PDBePISA (https://www.ebi.ac.uk/msd-srv/prot_int/cgi-bin/piserver) and PLIP (Adasme et al., 2021).

RESULTS AND DISCUSSION

Protein-Protein Docking of CUL4B-DDB1 to AhR

The 3D structure of CUL4B-DDB1 (PDB ID: 4A0L) before and after preparation is illustrated in Figures 1.a and 1.b. Two macromolecules, DDB2 and a 12BP DNA Duplex associated with the structure, were removed along with water. In 4A0L, the Rbx1 and DDB1 proteins were retained as they are subunits of the ubiquitin ligase complex essential for ubiquitination (Figures 1.c and 1.d). The original 3D structure of AhR (PDB ID: 5NJ8) contained an acetate ion, erbium ion, DNA, and aryl hydrocarbon receptor nuclear translocator, all were removed. Estradiol and Au, associated with the ERα structure (PDB ID: 1A52), were also removed to achieve a clean geometry (Figures 1.e and 1.f).

Protein-protein docking of CUL4B-DDB1 to AhR using ClusPro 2.0 resulted in 30 model structures with varying binding locations of AhR. AhR, a substrate receptor in the E3 ubiquitin ligase system (Dou et al., 2019; Luecke-Johansson et al., 2017), binds to DDB1 and recruits the substrate to function as an E3 ubiquitin ligase (Dou et al., 2019). Among these 30 models, structures CUL4B-DDB1-AhR 11, 13, and 25 demonstrated correct AhR binding regions (Figure 2). All models exhibited QMEAN scores below -4.0 and percentages of highly favored regions above 90% (Tables 1 and 2), indicating high-quality models (Studer et al., 2020; Williams et al., 2018). Based on the weighted score from ClusPro, QMEAN, MolProbity score, and the percentage of highly favored regions from Ramachandran plot analysis by SWISS-MODEL (Table 1 and 2), model 11 was determined to be the best among the three. Model 11 had more neighboring amino acid residues than models 13 and 25. Despite model 25 showing the highest percentage of highly favored regions in the Ramachandran plot, the overall parameters of model 11 outweighed those of the other models.

CUL4B-DDB1, as an E3 ubiquitin ligase complex, is known to bind to different substrate receptors. The well-known substrate receptor for CUL4B-DDB1 is cereblon, which targets thalidomide (Fischer et al., 2014). WDR3/WDR6, reported to be a substrate receptor that binds CUL4B-DDB1 in the ubiquitination of SPAK/OSR1 proteins (Dhiani & Mehellou, 2020), is another example.

Table 5. Energy binding affinity of *Acanthus ilicifolius* compounds to the CUL4B-DDB1-AhR-ERα protein complex

Rank	Name	Compound ID	Energy binding affinity (kcal/mol)
1	Acteoside	CID 5281800	-9.7
2	Isoacteoside	CID 6476333	-8.6
3	Acancifoliuside	-	-8.4
4	Acanthaminoside	-	-8.1
5	(-)-Lyoniresinol	CID 9888378	-7.7
6	(+)-Lyoniresinol-3a-O-β-glucopyranoside	-	-7.4
Native ligand	Estradiol	CID 5757	-8.9

Table 6. Interacting amino acid of acteoside with CUL4B-DDB1-AhR-ERα complex

Residue	Amino Acids	Distance (Å)
Hydrophobic interactions		
122C	Leucine	3.93
122C	Leucine	3.74
145C	Tyrosine	3.84
145C	Tyrosine	3.33
145C	Tyrosine	3.53
146C	Leucine	2.46
354A	Leucine	3.64
355A	Valine	3.70
Hydrogen bonds		
139C	Serine	2.27
139C	Serine	3.24
141C	Threonine	2.71
383A	Tryptophan	2.48
526A	Tyrosine	1.99

Table 7. PDBePISA parameter of CUL4B-DDB1-AhR-ERα protein complex in the absence or presence of ligand (acteoside)

CUL4B-DDB1-AhR-ERα				CUL4B-DDB1-AhR-ERα-ligand			
Interface Range	**ΔiG kcal/mol**	**N_{HB}**	**N_{SB}**	**Interface Range**	**ΔiG kcal/mol**	**N_{HB}**	**N_{SB}**
E:F	-17.8	25	13	E:F	-15.2	25	13
A:E	-4.1	29	29	A:E	-1.1	27	25
A:C	-14.8	14	14	A:C	-27.0	15	14

Note: A: ERa/DDB1; C: AhR; E: CUL4B; F: Rbx1 Structure; N_{HB}: Number of hydrogen bonds; N_{SB}: Number of salt bridges

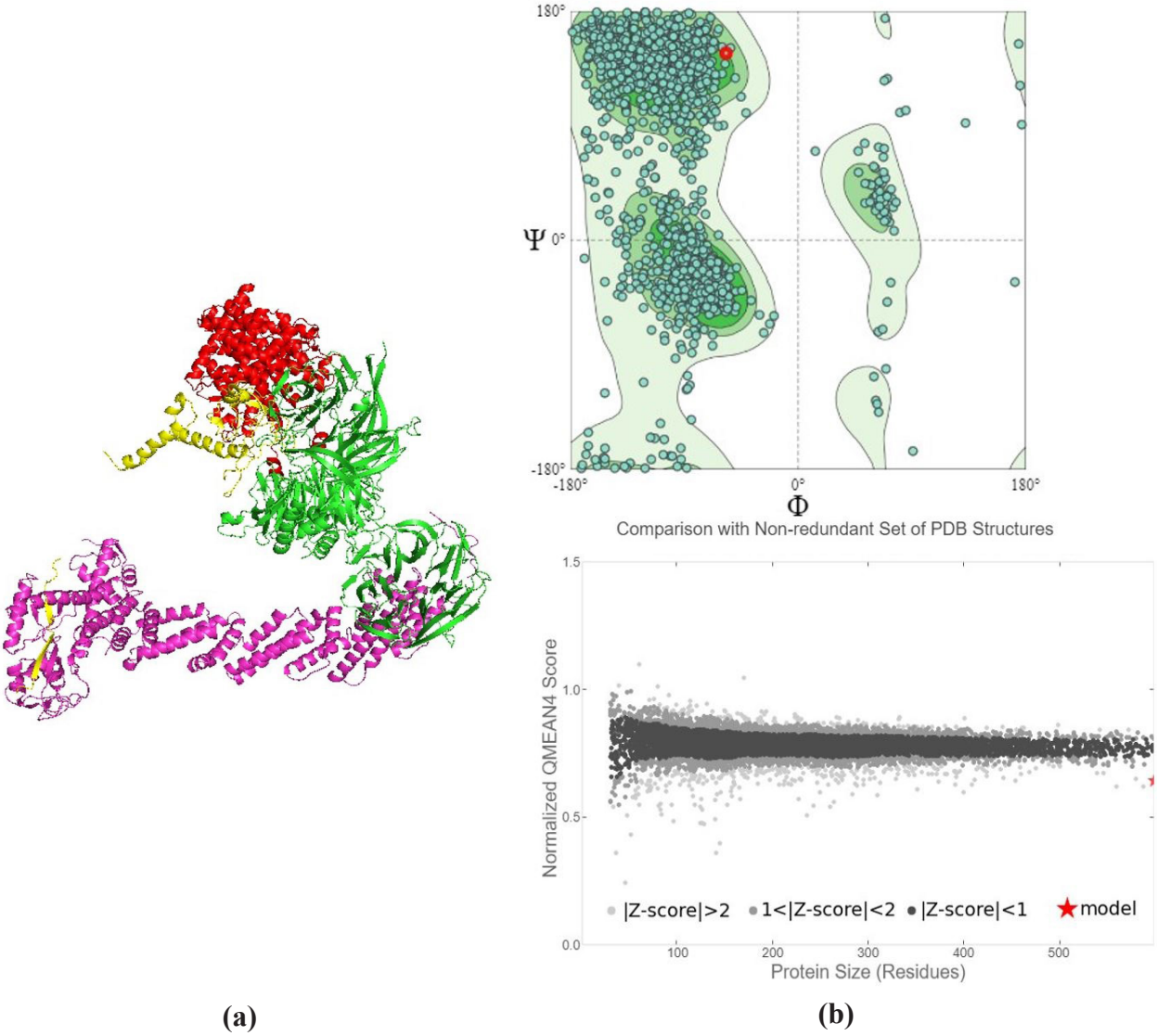

Figure 3. Visualization of complex CUL4B-DDB1-AhR-ERα model 0 (a) and its Ramachandran and quality comparison plots of the model generated from SWISS-MODEL analysis (b)

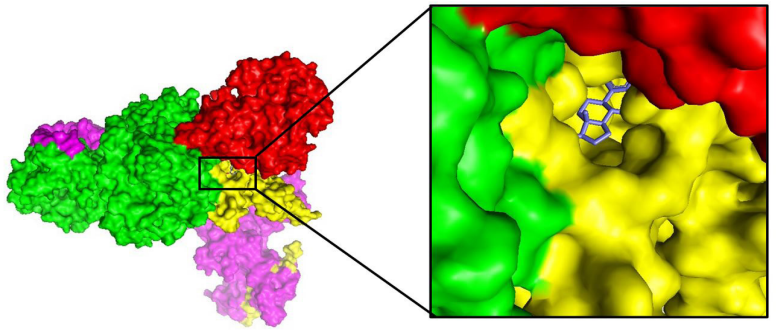

(a)

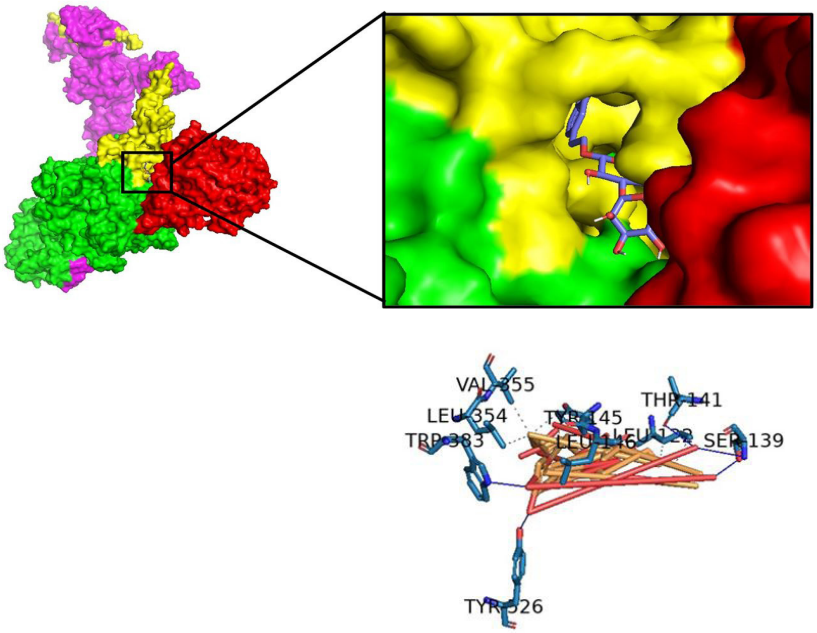

(b)

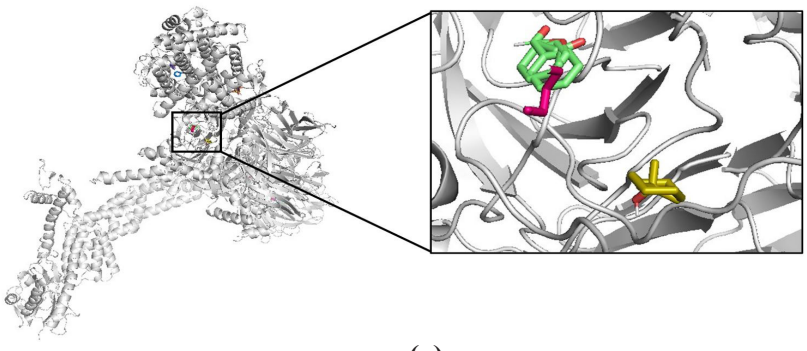

(c)

Figure 4. Model docking result of Acanthus ilicifolius compounds in CUL4B-DDB1-AhR-ERα. (a) estradiol and (b) acteoside which shows the interaction with amino acid residue of AhR and -ERα based on PLIP analysis. These bindings were occurred in the binding site as predicted based on FTMap analysis (c)

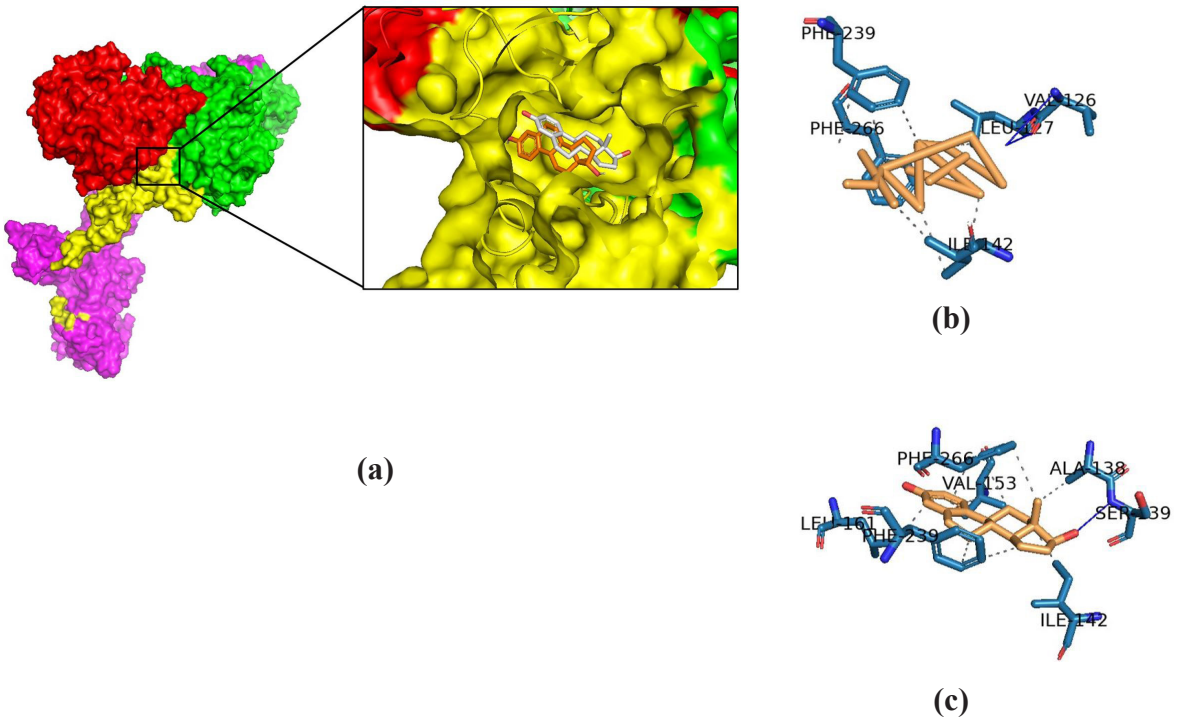

Figure 5. Superimposition of re-docked estradiol from native 1A52 (white) onto CUL4B-DDB1-AhR-ERα-estradiol (orange) complex in the binding site using PyMol (a) with the interacted amino acid residue shown based on PLIP analysis for native estradiol (b), and estradiol docked to CUL4B-DDB1-AhR-ERα (c)

Other studies have identified substrate receptors for CUL4B-DDB1, such as COP1 (Luo et al., 2023) and DCAF11 (Chen et al., 2017), among others (Jackson & Xiong, 2009). However, there is limited literature on AhR as a substrate receptor of CUL4B-DDB1, with only one report (Dou et al., 2019) since AhR was identified as an E3 ubiquitin ligase (Ohtake et al., 2009). Furthermore, no CUL4B-DDB1-AhR crystal structures are currently available in the PDB database.

Protein-protein docking of CUL4B-DDB1-AhR to ERα

In the protein-protein docking process, model 11 of the CUL4B-DDB1-AhR complex was used as the receptor in ClusPro 2.0, with ERα acting as the ligand. Protein-protein docking resulted in the generation of 18 models for the CUL4B-DDB1-AhR to ERα interaction. Model 0 emerged as the best representation of the CUL4B-DDB1-AhR-ERα structure, characterized by the correct ERα binding location, the highest number of members, and the lowest weighted score among the top five models (Table 3). According to PIC analysis, the interaction between AhR and ERα in the CUL4B-DDB1-AhR-ERα complex was identified at approximately amino acid 500 at the end of the C-terminal of the ERα ligand binding domain (LBD) (Table 4). This finding confirms the accurate binding location of ERα to the CUL4-DDB1-AhR complex (Figure 3) and supports the hypothesis presented in the only study investigating the association of ERα with the CUL4B ubiquitin complex (Ohtake et al., 2011; Huang et al., 2018).

***A. ilicifolius* compounds docking to the CUL4B-DDB1-AhR-ERα complex**

All six *A. ilicifolius* compounds and estradiol were used as ligands in ligand-protein docking targeting the CUL4B-DDB1-AhR-ERα complex. Docking was carried out using AutoDock Vina in PyRx 0.8. Acteoside and estradiol docked in the same binding pocket of the CUL4B-DDB1-AhR-ERα complex (Figure 4). These bindings occurred at the same site predicted by FTMap analysis (Figure 4.c). The energy binding affinities for all ligands are shown in Table 5. Docking validation involved re-docking estradiol from the native co-crystallized structure 1A52 to the CUL4B-DDB1-AhR-ERα complex, resulting in an RMSD value of 2.5 Å.

Considering the resolution of the native co-crystal structure 1A52 from the PDB is 2.8 Å, an RMSD below this number (between >2 Å and <3 Å) and the preservation of key residues indicate the validity of the docking protocol (Figure 5) (Carugo, 2003; Ramírez & Caballero, 2018).

Acteoside exhibited the lowest energy binding affinity among the *A. ilicifolius* compounds and estradiol, suggesting that it binds more strongly to the CUL4B-DDB1-AhR-ERα complex, than estradiol, the native ligand of ERα (Pantsar & Poso, 2018). Acteoside established hydrophobic interactions with CUL4B-DDB1-AhR-ERα residues at Leucine122, Tyrosine145, Leucine146 in AhR, and Leucine354, Leucine355 in ERα. Hydrogen bonds were also observed between acteoside and Serine 139, Threonine141 in AhR, and Tryptophan383, Tryptophan526 in ERα (Table 6). The binding of acteoside introduced several new amino acid residues that engage in hydrophobic interactions within the AhR-ERα interface region (Table 4). However, instead of weakening, the binding of acteoside in the CUL4B-DDB1-AhR-ERα complex strengthens the interaction between AhR and ERα. The binding of acteoside in the AhR-ERα interface region has been shown to weaken the interaction between CUL4B-Rbx1 and CUL4B-DDB1 (Table 7). The solvation-free energy increased in the interface region of CUL4B-Rbx1 and CUL4B-DDB1 after acteoside binding, weakening the interaction (Speight, 2020).

The Rbx1 protein is part of the Cullin-RING Ligase (CRL) complex, which is essential for CRL activities (Chen et al., 2015). Rbx1 recruits the E2 ubiquitin ligase, which then transfers ubiquitin to the substrate, promoting the ubiquitination of ERα. Therefore, a weakened interaction between Rbx1 and CUL4B could reduce or nullify the CUL4B-DDB1-AhR complex's ability to ubiquitinate and degrade ERα. This inhibition of ERα degradation supports the potential of acteoside as an antiosteoporosis agent. Acteoside has been reported to inhibit osteoclastogenesis by suppressing RANKL protein (Lee et al., 2013). Thus, the mechanism by which acteoside prevents osteoporosis by inhibiting ERα degradation via CUL4BAhR inhibition could be a novel approach to developing an antiosteoporosis agent.

CONCLUSION

Among the seven *Acanthus ilicifolius* compounds, acteoside exhibited the highest affinity towards the CUL4B-DDB1-AhR-ERα complex, surpassing estradiol, the native ligand. Acteoside strengthens the interaction between AhR and ERα but weakens the interaction between CUL4B, Rbx1, and DDB1. This weakened interaction is anticipated to hinder the ubiquitination of ERα. Therefore, acteoside is a promising candidate for antiosteoporosis, potentially inhibiting ERα degradation via CUL4BAhR. Biochemical, *in vitro*, and *in vivo* studies are required to substantiate this hypothesis further.

ACKNOWLEDGMENT

This research is funded by the General Directorate for Higher Education, Research and Technology (Dirjen Diktiristek) of the Ministry of Education, Culture, Research, and Technology (Kemendikbudristek) Republic of Indonesia under the scheme Penelitian Kerjasama Dalam Negeri year 2023 with contract number 182/E5/PG.02.00.PL/2023; 017/LL6/PB/AL.04/2023; A.11-III/230-S.Pj./LPPM/VI/2023.

CONFLICT OF INTEREST

The authors declare no conflict of interest.

REFERENCES

Adasme, M. F., Linnemann, K. L., Bolz, S. N., Kaiser, F., Salentin, S., Haupt, V. J., & Schroeder, M. (2021). PLIP 2021: expanding the scope of the protein–ligand interaction profiler to DNA and RNA. *Nucleic Acids Research*, *49*(W1), W530–W534. https://doi.org/10.1093/NAR/GKAB294

Bora, R., Adhikari, P. P., Das, A. K., Raaman, N., & Sharma, G. D. (2017). Ethnomedicinal, phytochemical, and, pharmacological aspects of genus acanthus. *International Journal of Pharmacy and Pharmaceutical Sciences*, *9*(12), 18. https://doi.org/10.22159/ijpps.2017v9i12.22386

Carugo, O. (2003). How root-mean-square distance (r.m.s.d.) values depend on the resolution of protein structures that are compared. *Journal of Applied Crystallography*, *36*(1), 125–128. https://doi.org/https://doi.org/10.1107/S0021889802020502

Chen, Z., Sui, J., Zhang, F., & Zhang, C. (2015). Cullin family proteins and tumorigenesis: genetic association and molecular mechanisms. *Journal of Cancer*, *6*(3), 233–242. https://doi.org/10.7150/jca.11076

Chen, Z., Wang, K., Hou, C., Jiang, K., Chen, B., Chen, J., Lao, L., Qian, L., Zhong, G., Liu, Z., Zhang, C., & Shen, H. (2017). CRL4BDCAF11 E3 ligase targets p21 for degradation to control cell cycle progression in human osteosarcoma cells. *Scientific Reports*, *7*(1), 1175. https://doi.org/10.1038/s41598-017-01344-9

Dallakyan, S., & Olson, A. J. (2015). Small-molecule library screening by docking with PyRx. *Methods in Molecular Biology*. https://doi.org/10.1007/978-1-4939-2269-7_19

Dhiani, B. A., & Andini, P. M. (2021). *Penentuan Aktivitas Estrogenik Subfraksi dari Fraksi Air Daun Jeruju (Acanthus ilicifolius L.) dengan Metode E- Screen Assay*. Universitas Muhammadiyah Purwokerto.

Dhiani, B. A., & Mehellou, Y. (2020). The Cul4-DDB1-WDR3/WDR6 complex binds SPAK and OSR1 kinases in a phosphorylation-dependent manner. *ChemBioChem*, *21*(5). https://doi.org/10.1002/cbic.201900454

Dou, H., Duan, Y., Zhang, X., Yu, Q., Di, Q., Song, Y., Li, P., & Gong, Y. (2019). Aryl hydrocarbon receptor (AhR) regulates adipocyte differentiation by assembling CRL4B ubiquitin ligase to target PPARγ for proteasomal degradation. *Journal of Biological Chemistry*, *294*(48), 18504–18515. https://doi.org/10.1074/JBC.RA119.009282

Fischer, E. S., Bohm, K., Lydeard, J. R., Yang, H., Stadler, M. B., Cavadini, S., Nagel, J., Serluca, F., Acker, V., Lingaraju, G. M., Tichkule, R. B., Schebesta, M., Forrester, W. C., Schirle, M., Hassiepen, U., Ottl, J., Hild, M., Beckwith, R. E., Harper, J. W., … Thoma, N. H. (2014). Structure of the DDB1-CRBN E3 ubiquitin ligase in complex with thalidomide. *Nature*, *512*(7512), 49–53

Hendrijatini, N., Rostiny, R., Kurdi, A., Ari, M. DA, Sitalaksmi, Ratri Maya Hapsari, P. D., Arief, V. V, & Sati, P. Y. (2019). Molecular triad RANK/ RANKL/ OPG in mandible and femur of wistar rats (*Rattus norvegicus*) with type 2 diabetes mellitus. *Recent Advances in Biology and Medicine*, *5*, 1–7. https://www.rcsb.org/. (2022). *RCSB PDB: Homepage*. https://www.rcsb.org/

Huang, W., Peng, Y., Kiselar, J., Zhao, X., Albaqami, A., Mendez, D., Chen, Y., Chakravarthy, S., Gupta, S., Ralston, C., Kao, H.-Y., Chance, M. R., & Yang, S. (2018). Multidomain architecture of estrogen receptor reveals interfacial cross-talk between its DNA-binding and ligand-binding domains. *Nature Communications*, *9*(1), 3520. https://doi.org/10.1038/s41467-018-06034-2

Jackson, S., & Xiong, Y. (2009). CRL4s: the CUL4-RING E3 ubiquitin ligases. *Trends in Biochemical Sciences*, *34*(11), 562. https://doi.org/10.1016/J.TIBS.2009.07.002

Jia, M., Nie, Y., Cao, D. P., Xue, Y. Y., Wang, J. S., Zhao, L., Rahman, K., Zhang, Q. Y., & Qin, L. P. (2012). Potential antiosteoporotic agents from plants: A comprehensive review. *Evidence-Based Complementary and Alternative Medicine*, *2012*. https://doi.org/10.1155/2012/364604

Jungsukcharoen, J., Dhiani, B. A., Cherdshewasart, W., Vinayavekhin, N., Sangvanich, P., & Boonchird, C. (2014). *Pueraria mirifica* leaves, an alternative potential isoflavonoid source. *Bioscience, Biotechnology and Biochemistry*, *78*(6). https://doi.org/10.1080/09168451.2014.910091

Khalid, A. B., & Krum, S. A. (2016). Estrogen receptors alpha and beta in bone. *Bone*, *87*, 130. https://doi.org/10.1016/J.BONE.2016.03.016

Kozakov, D., Grove, L. E., Hall, D. R., Bohnuud, T., Mottarella, S. E., Luo, L., Xia, B., Beglov, D., & Vajda, S. (2015). The FTMap family of web servers for determining and characterizing ligand-binding hot spots of proteins. *Nature Protocols*. https://doi.org/10.1038/nprot.2015.04

Kozakov, D., Hall, D. R., Xia, B., Porter, K. A., Padhorny, D., Yueh, C., Beglov, D., & Vajda, S. (2017). The ClusPro web server for protein–protein docking. *Nature Protocols*, *12*, 255. https://doi.org/10.1038/nprot.2016.169.https://www.nature.com/articles/nprot.2016.169#supplementary-information

Lee, J., & Zhou, P. (2012). Pathogenic role of the crl4 ubiquitin ligase in human disease. *Frontiers in Oncology*, *2*(MAR). https://doi.org/10.3389/FONC.2012.00021

Lee, S. Y., Lee, K. S., Yi, S. H., Kook, S. H., & Lee, J. C. (2013). Acteoside suppresses RANKL-Mediated osteoclastogenesis by inhibiting c-Fos induction and NF-κB pathway and attenuating ROS production. *PLOS ONE*, *8*(12), e80873. https://doi.org/10.1371/JOURNAL.PONE.0080873

Luecke-Johansson, S., Gralla, M., Rundqvist, H., Ho, J. C., Johnson, R. S., Gradin, K., & Poellinger, L. (2017). A molecular mechanism to switch the aryl hydrocarbon receptor from a transcription factor to an E3 ubiquitin ligase. *Molecular and Cellular Biology*, *37*(13). https://doi.org/10.1128/MCB.00630-16

Luo, D., Chen, M., Li, Q., Wang, K., Wang, K., Li, J., Fu, G., Shan, Z., Liu, Q., Yang, Y., Liang, L., Ma, Y., Qin, Y., Qin, J., Gao, D., & Li, X. (2023). CUL4B-DDB1-COP1-mediated UTX downregulation promotes colorectal cancer progression. *Experimental Hematology & Oncology*, *12*(1), 77. https://doi.org/10.1186/s40164-023-00440-z

Ohtake, F., Fujii-Kuriyama, Y., & Kato, S. (2009). AhR acts as an E3 ubiquitin ligase to modulate steroid receptor functions. *Biochemical Pharmacology*, *77*(4), 474–484. https://doi.org/10.1016/J.BCP.2008.08.034

Ohtake, F., Fujii-Kuriyama, Y., Kawajiri, K., & Kato, S. (2011). Cross-talk of dioxin and estrogen receptor signals through the ubiquitin system. *The Journal of Steroid Biochemistry and Molecular Biology*, *127*(1–2), 102–107. https://doi.org/10.1016/J.JSBMB.2011.03.007

Pantsar, T., & Poso, A. (2018). Binding affinity via docking: fact and fiction. *Molecules (Basel, Switzerland)*, *23*(8). https://doi.org/10.3390/molecules23081899

Ramírez, D., & Caballero, J. (2018). Is it reliable to take the molecular docking top scoring position as the best solution without considering available structural data?. *Molecules*, *23*(5). https://doi.org/10.3390/molecules23051038

Salari, N., Ghasemi, H., Mohammadi, L., Behzadi, M. hasan, Rabieenia, E., Shohaimi, S., & Mohammadi, M. (2021). The global prevalence of osteoporosis in the world: a comprehensive systematic review and meta-analysis. *Journal of Orthopaedic Surgery and Research*, *16*(1), 1–20. https://doi.org/10.1186/S13018-021-02772-0/FIGURES/8

Saranya, A., Ramanathan, T., Kesavanarayanan, K. S., & Adam, A. (2015). Traditional medicinal uses, chemical constituents and biological activities of a mangrove plant, *Acanthus ilicifolius* Linn. : A brief review. *American-Eurasian Journal of Agricultural & Environmental Sciences, 15*(2), 243–250. https://doi.org/10.5829/idosi.aejaes.2015.15.2.12529

Shen, Y., Huang, X., Wu, J., Lin, X., Zhou, X., Zhu, Z., Pan, X., Xu, J., Qiao, J., Zhang, T., Ye, L., Jiang, H., Ren, Y., & Shan, P.-F. (2022). The global burden of osteoporosis, low bone mass, and its related fracture in 204 countries and territories, 1990-2019. *Frontiers in Endocrinology*, *13*, 882241. https://doi.org/10.3389/fendo.2022.882241

Singh, D., & Aeri, V. (2013). Phytochemical and pharmacological potential of *Acanthus ilicifolius*. *Journal of Pharmacy and Bioallied Sciences*, *5*(1), 17–20. https://doi.org/10.4103/0975-7406.106557

Speight, J. G. (2020). Water chemistry. *Natural Water Remediation*, 91–129. https://doi.org/10.1016/B978-0-12-803810-9.00003-6

Streicher, C., Heyny, A., Andrukhova, O., Haigl, B., Slavic, S., Schüler, C., Kollmann, K., Kantner, I., Sexl, V., Kleiter, M., Hofbauer, L. C., Kostenuik, P. J., & Erben, R. G. (2017). Estrogen regulates bone turnover by targeting RANKL expression in bone lining cells. *Scientific Reports*, *7*(1), 1–14. https://doi.org/10.1038/s41598-017-06614-0

Studer, G., Studer, G., Rempfer, C., Rempfer, C., Waterhouse, A. M., Waterhouse, A. M., Gumienny, R., Gumienny, R., Haas, J., Haas, J., Schwede, T., & Schwede, T. (2020). QMEANDisCo—distance constraints applied on model quality estimation. *Bioinformatics*, *36*(8), 2647–2647. https://doi.org/10.1093/BIOINFORMATICS/BTAA058

Tina, K. G., Bhadra, R., & Srinivasan, N. (2007). PIC: Protein Interactions Calculator. *Nucleic Acids Research*, *35*(suppl_2), W473–W476. https://doi.org/10.1093/nar/gkm423

Van Kiem, P., Quang, T. H., Huong, T. T., Nhung, L. T. H., Cuong, N. X., Van Minh, C., Choi, E. M., & Kim, Y. H. (2008). Chemical constituents of *Acanthus ilicifolius* L. and effect on osteoblastic MC3T3E1 cells. *Archives of Pharmacal Research*, *31*, 823–829.

WHO. (2023). *Ageing and health*. https://www.who.int/news-room/fact-sheets/detail/ageing-and-health

Williams, C. J., Headd, J. J., Moriarty, N. W., Prisant, M. G., Videau, L. L., Deis, L. N., Verma, V., Keedy, D. A., Hintze, B. J., Chen, V. B., Jain, S., Lewis, S. M., Arendall III, W. B., Snoeyink, J., Adams, P. D., Lovell, S. C., Richardson, J. S., & Richardson, D. C. (2018). MolProbity: More and better reference data for improved all-atom structure validation. *Protein Science*, *27*(1), 293–315. https://doi.org/https://doi.org/10.1002/pro.3330

Wu, M., Lai, H., Deng, Q., Peng, X., Shen, J., Zhou, X., Peng, W., Zhu, L., Tu, H., & Li, X. (2022). The evaluation of xiaozeng qianggu tablets for treating postmenopausal osteoporosis via up-regulated autophagy. *Evidence-Based Complementary and Alternative Medicine*, *2022*. https://doi.org/10.1155/2022/3960834